

Arthur R. C. McCray
Physics, Carleton College
PARADIM Research Accomplishments Paper
8/3/16

Title: Orientational Disorder in Epitaxially Connected Quantum Dot Solids

Abstract:

Lattices of fused PbSe quantum dots offer interesting possibilities for the manufacturing of films with tunable electronic properties. However, theoretically predicted electronic properties are not yet realizable due to disorder in the films. Using STEM imaging techniques we analyze the orientational component of the disorder in these lattices. We characterize the misalignment between each dot's atomic lattice and the larger quantum dot superlattice as well as the atomic lattices of its neighbors. We find that the superlattice structure near highly misoriented dots is more disordered than in other parts of the lattice, and that individual dots prefer to align to the orientation of their neighbors rather than the superlattice. Furthermore, dots that are aligned with the plane of the film are always well aligned to their neighbors, while a statistically significant fraction of dots which are misoriented from the film plane misalign from their neighbors by 45 degrees.

Introduction:

Quantum dots (QDs) are semiconductor nanocrystals often suspended as colloids in a solution. They range in size from 4 to 12 nanometers (nm) in diameter, and display interesting and potentially useful properties. When doped they behave much like a particle in a box by having discrete allowable energy states, and QDs are therefore sometimes referred to as "artificial atoms". There are a variety of exciting applications for quantum dots including quantum computers, displays, and transparent solar cells.

Lead selenide (PbSe) colloidal QDs can be assembled into micron scale square superlattices (SLs) in which the rock salt atomic structure of the QDs are aligned with the SL. Theoretical research of these systems predicts films with highly tunable band structures allowing for the fabrication of materials with customizable electronic properties [1-3]. The process of fabricating these films is via self-assembly at a liquid-liquid interface, in which colloidal PbSe QDs are assembled on a liquid substrate into a hexagonal lattice. Subsequent chemical treatment removes organic ligands from the $\langle 100 \rangle$ facets causing the dots to rotate, reorient, and fuse, while the SL simultaneously restructures into a square epitaxially connected superlattice through this oriented attachment process.

The electronic properties of these films are limited, however, by disorder within the SL of QDs which prevents electron delocalization and must be understood before ideal films can be made. SL disorder originates during the film formation process, and in particular by the restructuring of the SL in response to the reorientation and attachment of individual QDs. This process has therefore been the focus of significant scientific interest [4,5], and yet remains poorly understood. We therefore examined how the orientation of the atomic lattice (AL) relates to

surrounding SL structure in order to directly experimentally and statistically explore the connection between the superlattice structure and the oriented attachment process.

Methods:

Using aberration corrected scanning transmission electron microscopy (STEM) we directly observed both the atomic lattice and superlattice structure of epitaxially connected lead selenide (PbSe) QD solids. The images analyzed were high angle annular dark field (HAADF) images with 160 nm field of view and resolution such that the atomic lattice orientation was visible (Fig. 1).

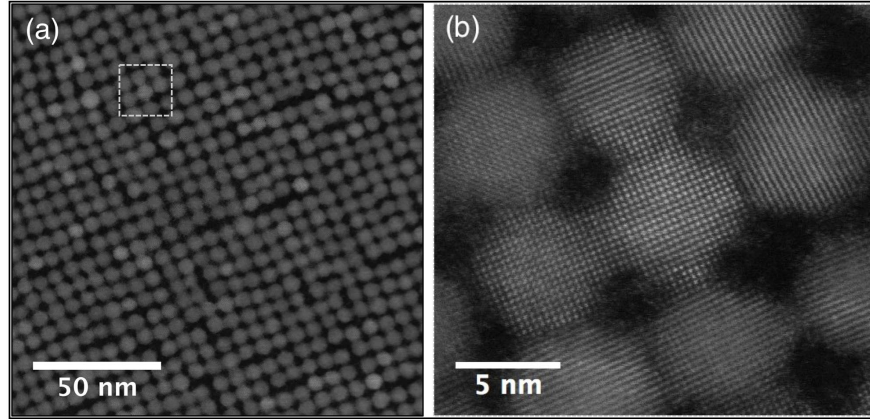


Figure 1: STEM HAADF images of epitaxially connected PbSe quantum dots at superlattice (a) and atomic (b) scales.

The majority of our work is based on the orientations and placement of each QD. Atomic lattice orientation was determined for each individual QD by extracting the locations of each QD in an image, taking the fast Fourier transform (fft) of single isolated dots, and identifying the direction in k-space of the Bragg spots. This process was performed using our own in-house algorithms, described in detail below.

To identify each individual dot we used a watershed segmentation initially, followed by a manual proofing to correct any mistakes. We then determined QD centroid positions by calculating the center of mass of each segmented QD. Once centroid positions were identified, we estimate the local symmetry of the superlattice by calculating Ψ_4 for each QD, a metric defined as

$$\Psi_4 = \frac{1}{n} \sum_{j=1}^n e^{4i\theta_j}, \quad (1)$$

where n is the number of neighbors and θ_j the angle of the line between the dot and the neighbor j . Taking the magnitude of the complex number, $|\Psi_4|$, we get a real scalar between 0 and 1 (0 being no symmetry and 1 being perfect four-fold symmetry) that quantifies how square the superlattice is around that dot. Additionally, the phase of Ψ_4 encodes the direction of best four-fold symmetry around a dot. Letting $\beta = \arg(\Psi_4)$, we obtain a metric of the local orientation of

the superlattice around the dot. Furthermore, by averaging the local orientation β of all the dots in a lattice we get one way of defining a global SL orientation, $\langle\beta\rangle$.

Because Ψ_4 is defined based on the placement of a dot's neighbors, one can calculate it in multiple ways depending on how "neighboring" QDs are defined. The first method we used defines a dot's "neighbors" to be all dots within a certain distance determined heuristically. In this first method we define

$$\Psi_{4KD} = \frac{1}{n} \sum_{j=1}^n e^{4i\theta_j}, \quad (2)$$

where the sum is over all dots within the specified distance.

The second method we used to calculate Ψ_4 involves first constructing a Voronoi diagram, which partitions the image into regions defined as the set of all points closest to a single QD centroid. This allows us to define "neighbors" as dots whose Voronoi cells share an edge. We then weight the neighbors based on the edge length so that nearer dots are weighted more. Thus

$$\Psi_{4Vor} = \frac{1}{L} \sum_{j=1}^n l_j * e^{4i\theta_j}, \quad (3)$$

where L is the total perimeter of the Voronoi cell and l_j is the edge length shared with neighbor j .

We find that Ψ_{4Vor} tells us more about the surrounding superlattice structure of a dot, and often includes neighbors which aren't bonded. In contrast, by using a conservative cutoff distance we find that Ψ_{4KD} of a dot tells us about the symmetry of bonded dots only. In both cases, Ψ_{4KD} and Ψ_{4Vor} , we obtain a direction β^{KD} and β^{Vor} , respectively, which is a metric of the local superlattice orientation, as well as a magnitude which quantifies how four-fold symmetric the surrounding superlattice is.

From these orientations we calculated the angles by which each dot is misaligned from the local and global SL orientation, $(\alpha^{\beta^{KD}}/\alpha^{\beta^{Vor}})$, and $(\alpha^{\langle\beta^{KD}\rangle}/\alpha^{\langle\beta^{Vor}\rangle})$, respectively. Furthermore, we can compare the orientation of the QD to that of its neighbors, and get " $\alpha - \langle\alpha\rangle_n$ ", which is the average misalignment of a QD from its neighbors.

Results and Discussion:

The vertical axis of Figure 2 shows the misalignment $\alpha^{\langle\beta^{Vor}\rangle}$ of each dot's atomic lattice from the mean superlattice angle $\langle\beta^{Vor}\rangle$. The horizontal axis shows the misalignment between the local superlattice angle β^{Vor} and the mean superlattice angle $\langle\beta^{Vor}\rangle$. Each point in the scatterplot thus indicates how well the local superlattice and local atomic lattice directions align for a single QD in a typical image. Finding a best fit line to only the central cluster of well-aligned datapoints, we see a slope of 0.24 which indicates that if the local superlattice around a dot is misaligned from the global SL, the dot's atomic lattice will most likely be misaligned in that direction as well. Thus the local superlattice "pull's" the AL orientation away from the mean superlattice direction.

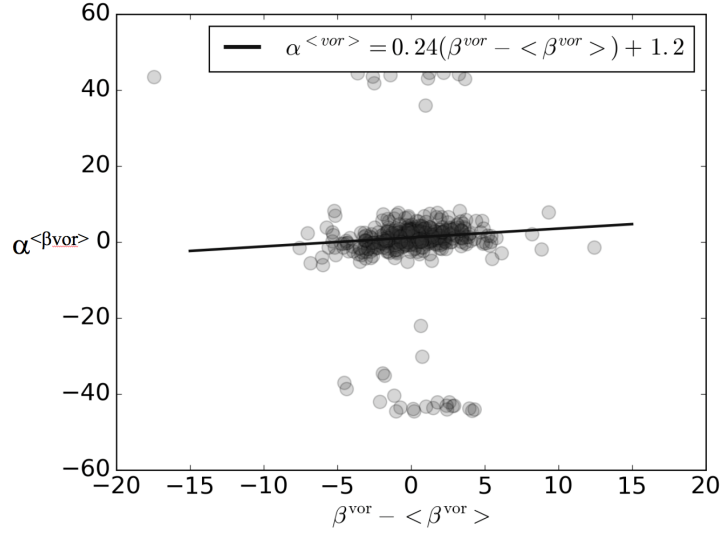


Figure 2: Dots with a local superlattice, β^{vor} , more misaligned from the average local superlattice, $\langle\beta^{vor}\rangle$ (a measure of global SL orientation), are more likely to have their atomic lattice, $\alpha^{<\beta^{vor}>}$, be misaligned in the same direction.

Knowing that a QDs orientation is determined at least in part by its local SL structure, we now turn to examine that dot's neighbor's orientations as well. Limiting the image to dots that are well aligned with the local superlattice, ($\alpha^{\beta^{vor}} < 15$), we can examine trends in dots that are aligning at least close to that of an ideal film. Figure 3a is a histogram of these QDs misalignment from the mean orientation of its nearest neighbors ($\alpha - \langle\alpha\rangle_n$), and Fig. 3b a histogram of the dots' misalignment from their local superlattice, $\alpha^{\beta^{vor}}$. We find that the QDs misalignment from their neighbors has a tighter distribution than their misalignments from the superlattice, shown by the difference in standard deviations $\sigma_{<\alpha>} = 1.73$ and $\sigma_{\beta^{vor}} = 3.08$, respectively. From this we conclude that the QDs orientation is more dependent on the orientations of its neighbors than the local superlattice structure that surrounds it.

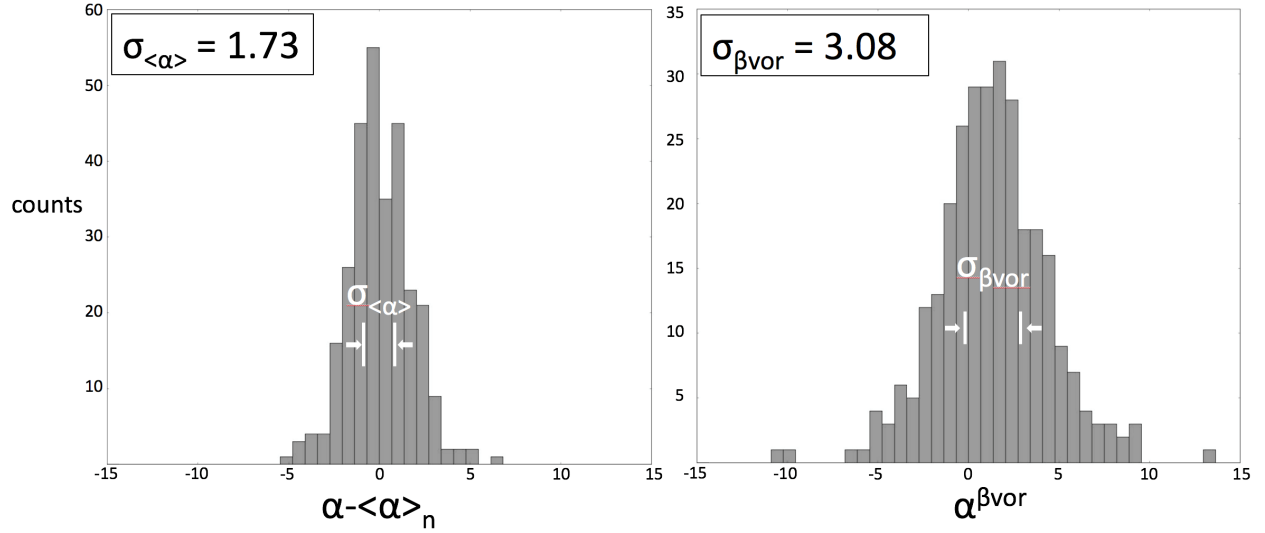


Figure 3: Histogram of the misalignments from neighbors (a), and from local SL (b) of dots that are well aligned with the superlattice, ($\alpha^{\beta_{vor}} < 15$). The distribution of $\alpha - \langle \alpha \rangle_n$ indicates that the QDs prefer to align with the orientation of their neighbors than with the local SL.

While that applies to dots that are relatively well aligned with the superlattice, we also care about those that are not. Figure 4 compares histograms of $|\Psi_{4Vor}|$ for dots that are well-aligned with their local superlattice, $\alpha^{\beta_{vor}} < 15$ (Fig. 4a), and misaligned $\alpha^{\beta_{vor}} > 15$ (Fig. 4b). We see that well aligned dots have a smooth distribution of $|\Psi_{4Vor}|$ values with a peak at approximately 0.7 and dying off rapidly near 0. In contrast, the distribution of $|\Psi_{4Vor}|$ values for misaligned dots is approximately uniform, with a mean of ~ 0.5 and a significant fraction with small $|\Psi_{4Vor}|$ values. Physically, this indicates that local superlattice disorder accompanies significant misalignment of the atomic lattice. This may have important implications for the origins of superlattice disorder during the oriented attachment process.

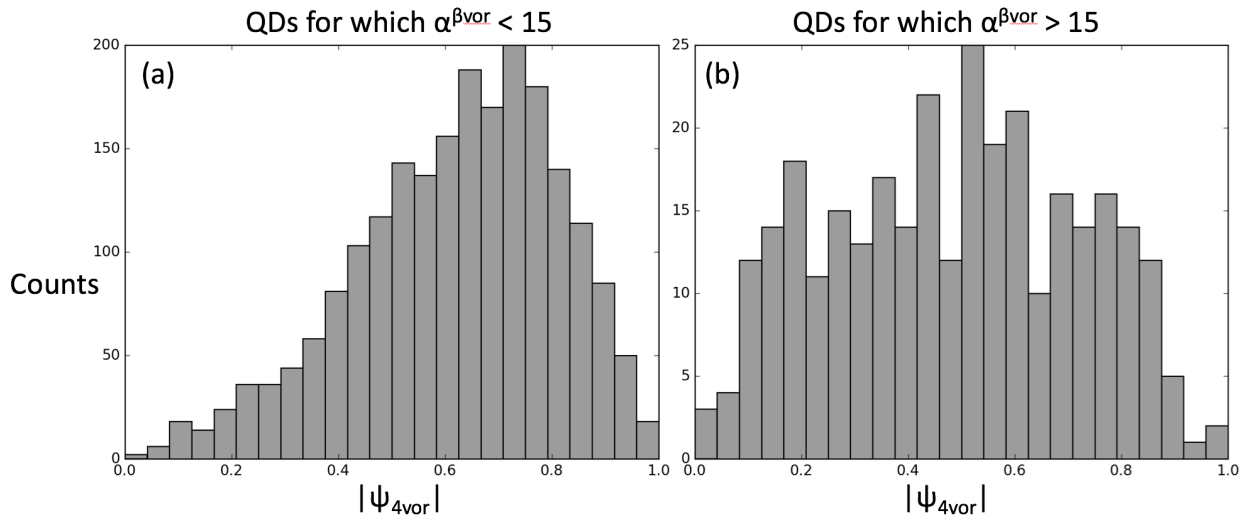


Figure 4: Histograms of the magnitude of $|\Psi_{4Vor}|$ for dots with atomic lattices well aligned to

the local superlattice (a) and misaligned from the local superlattice (b). A larger $|\Psi_{4vor}|$ value equates to a more four-fold symmetric local superlattice for a dot. Dots that are very misaligned from the superlattice occur in regions where the superlattice is more disordered.

Thus far we have only discussed QD alignment in the plane of the lattice. However, we can also draw conclusions about QD orientation in the out of plane direction. Dots oriented with $\langle 100 \rangle$ facets pointed perpendicular to the plane (which they all should as predicted by molecular dynamics research [1]) are identifiable by square atomic lattice structure in our images. Similarly, dots oriented in the $\langle 110 \rangle$ direction are identifiable by an asymmetrical hexagonal lattice due to the projection nature of STEM imaging. We find these $\langle 110 \rangle$ oriented dots make up less than 1% of the total dots. Finally, dots that are oriented between the $\langle 100 \rangle$ and $\langle 110 \rangle$ directions appear to have lattice fringes in only a single direction again due to the projection imaging process. They are oriented between the $\langle 100 \rangle$ and $\langle 110 \rangle$ directions, so we refer to these dots as lying in a $\langle 1n0 \rangle$ orientation (Fig. 5a).

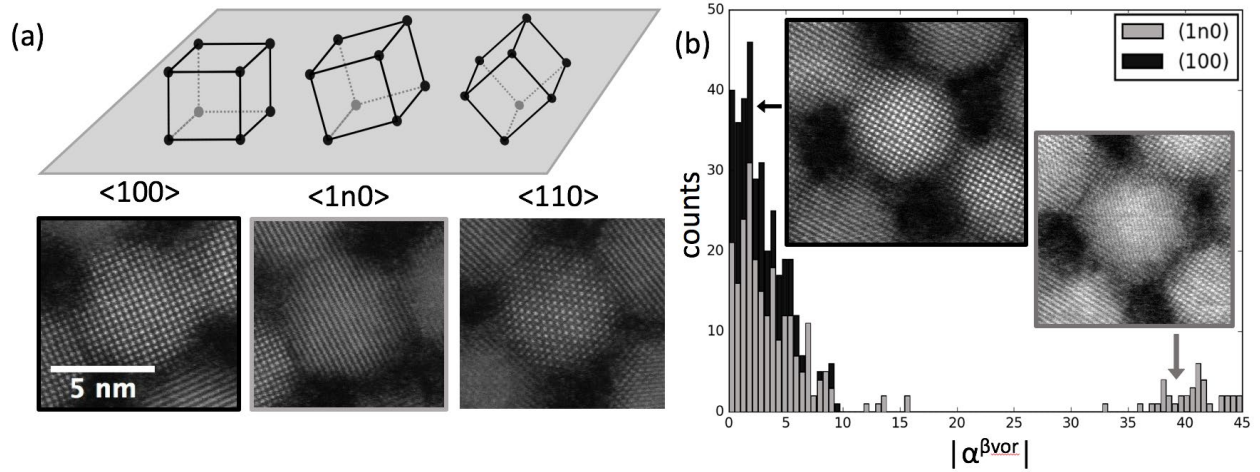


Figure 5: A cartoon of the crystal orientation of QDs oriented in the $\langle 100 \rangle$, $\langle 1n0 \rangle$, and $\langle 110 \rangle$ orientations with examples taken from a HAADF STEM image (a), and histogram of misorientation from the local superlattice $\alpha^{\beta vor}$ with examples of aligned and misaligned dots (b). Distinguishing between dots of $\langle 100 \rangle$ and $\langle 1n0 \rangle$ orientations shows that all highly misaligned dots ($\alpha^{\beta vor} > 10$) are in the $\langle 1n0 \rangle$ orientation and misaligned out of the SL plane as well.

In Figure 5b we show a histogram of the magnitude of misalignment, $|\alpha^{\beta vor}|$, of dots from the local superlattice while distinguishing dots of $\langle 100 \rangle$ and $\langle 1n0 \rangle$ orientations. We find that all of the very misaligned QDs, ($|\alpha^{\beta vor}| > 15$), are also misaligned out of plane in the $\langle 1n0 \rangle$ direction (Fig. 5b). Furthermore, the misaligned dots are centered around 45 degrees implying there is a favorable energy state for dots that are out of plane somewhat and offset from their neighbors by 45 degrees.

Conclusions:

Our work shows that when forming these PbSe superlattices, the most important thing that determines the alignment of a dot's atomic lattice is the orientations of the AL of its neighboring dots. While the QDs do like to align in the direction of their local SL it is a much smaller factor and dots prefer to be aligned with neighbors, even at the expense of misalignment from the SL.

We have also showed that if a dot is oriented correctly in the plane of the film then it will be fairly well aligned ($|\alpha^{avor}| < 10$) with the local SL as well. However, if the dot is oriented between $\langle 100 \rangle$ and $\langle 110 \rangle$ then its orientation is less predictable. Furthermore, for the $\langle 1n0 \rangle$ dots there appears to be a favorable energy state when the dot is oriented 45 degrees off of its local SL.

Finally, the dots that are heavily misaligned from their neighbors for the most part have lower $|\Psi_{4Vor}|$. One can generalize that if a dot is misaligned from its neighbors than it is more likely to occur in parts of the lattice that are distorted, missing dots, or otherwise not square.

The QDs misorientations and misalignments are results of the oriented attachment process by which these films are formed. Hopefully these insights will allow for a greater understanding of this process and lead to the fabrication of more ideal quantum dot films.

Acknowledgements:

I'd like to thank my mentor, Ben Savitzky, for all of the help he has given me; I wouldn't have been able to do this research without him. I'd also like to thank my PI, Lena Kourkoutis, for the continued support and everything she's taught me.

This material is based upon work supported by the National Science Foundation (Platform for the Accelerated Realization, Analysis, and Discovery of Interface Materials (PARADIM) under Cooperative Agreement No. DMR-1539918.) This work made use of the Cornell Center for Materials Research Shared Facilities which are supported through the NSFMRSEC program (DMR-1120296).

References:

- [1] Lazarenkova, O. L.; Balandin, A. A. *J. Appl. Phys.* **2001**, *89* (10), 5509–5515.
- [2] Kalesaki, E.; Evers, W. H.; Allan, G.; Vanmaekelbergh, D.; Delerue, C. *Phys. Rev. B - Condens. Matter Mater. Phys.* **2013**, *88* (11), 1–9.
- [3] Park, C.-H.; Louie, S. G. *Nano Lett.* **2009**, *9* (5), 1793–1797.
- [4] Schapotschnikow, P.; van Huis, M. A.; Zandbergen, H. W.; Vanmaekelbergh, D.; Vlugt, T. J. H. *Nano Lett.* **2010**, (10), 3966–3971.
- [5] van Huis, M. A.; Kunneman, L. T.; Overgaag, K.; Xu, Q.; Pandraud, G.; Zandbergen, H. W., & Vanmaekelbergh, D. *Nano lett.* **(2008)**, *8*(11), 3959-3963.

If this ends up being converted to two column, here are a few alternative layouts of some of the figures.

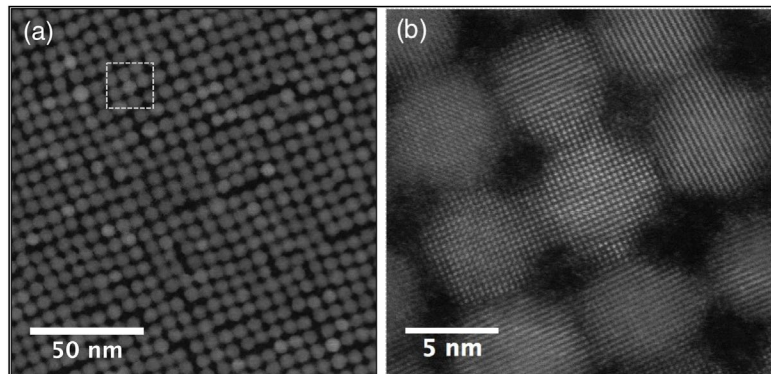


Figure 1: STEM HAADF images of epitaxially connected PbSe quantum dots at superlattice (a) and atomic (b) scales.

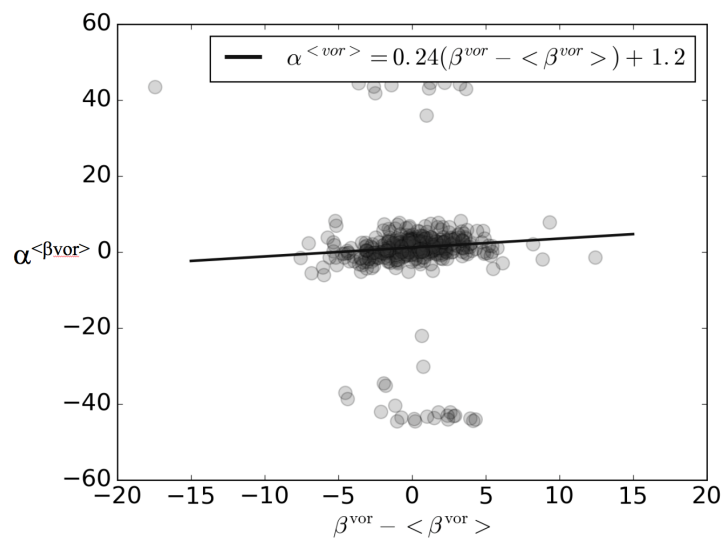


Figure 2: Dots with a local superlattice, β^{vor} , more misaligned from the average local superlattice, $\langle \beta^{vor} \rangle$ (a measure of global SL orientation), are more likely to have their atomic lattice, $\alpha^{\langle \beta^{vor} \rangle}$, be misaligned in the same direction.

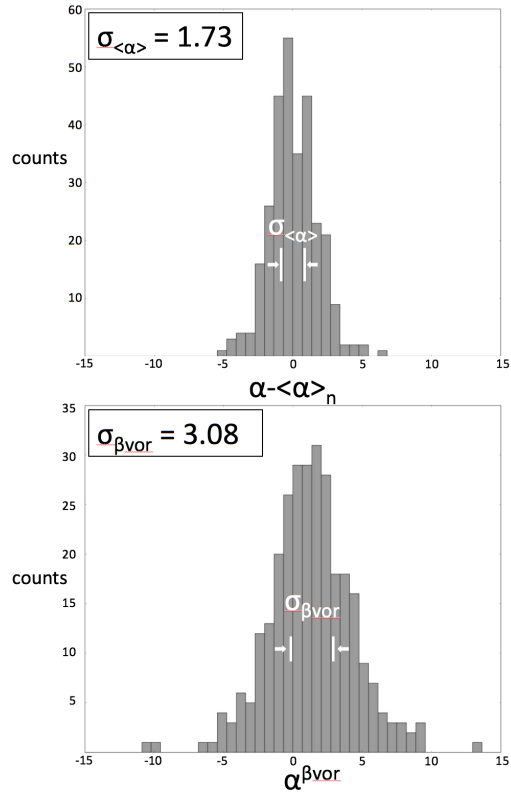


Figure 3: Histogram of the misalignments from neighbors (a), and from local SL (b) of dots that are well aligned with the superlattice, ($\alpha^{\beta_{vor}} < 15$). The distribution of $\alpha - \langle \alpha \rangle_n$ indicates that the QDs prefer to align with the orientation of their neighbors than with the local SL.

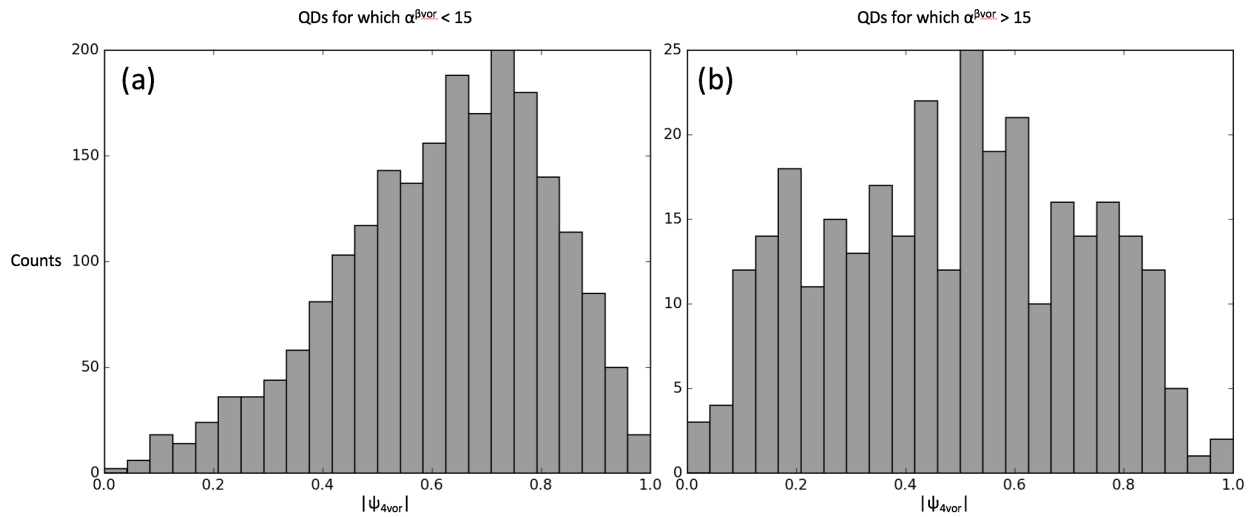


Figure 4: Histograms of the magnitude of $|\Psi_{4Vor}|$ for dots with atomic lattices well aligned to the local superlattice (a) and misaligned from the local superlattice (b). A larger $|\Psi_{4Vor}|$ value equates to a more four-fold symmetric local superlattice for a dot. Dots that are very misaligned from the superlattice occur in regions where the superlattice is more disordered.

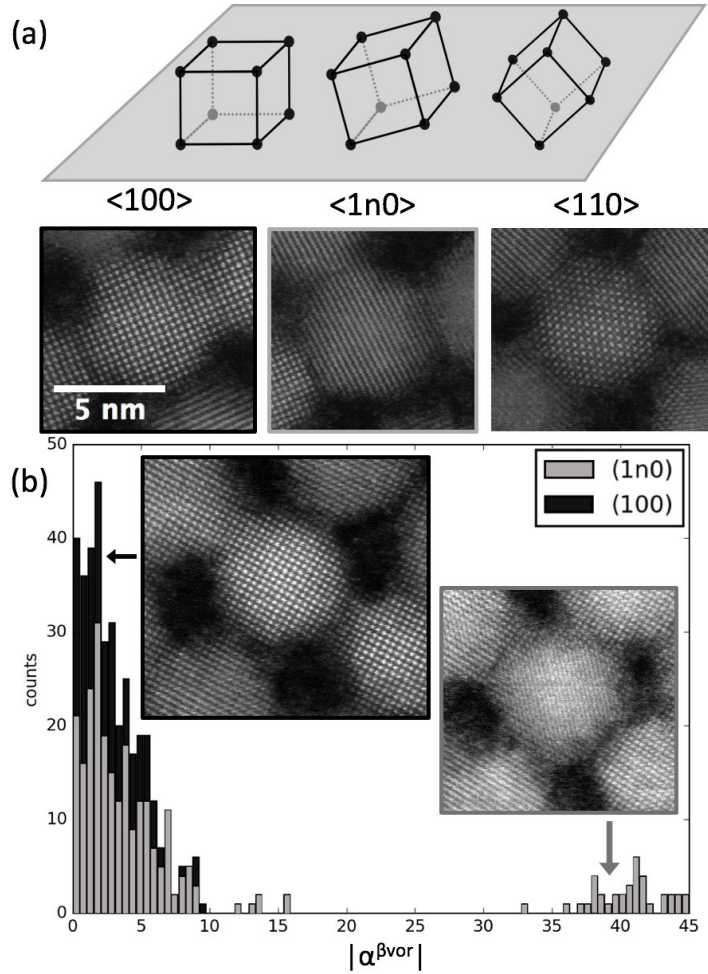


Figure 5: A cartoon of the crystal orientation of QDs oriented in the $\langle 100 \rangle$, $\langle 1n0 \rangle$, and $\langle 110 \rangle$ orientations with examples taken from a HAADF STEM image (a), and histogram of misorientation from the local superlattice $\alpha^{\beta_{\text{vor}}}$ with examples of aligned and misaligned dots (b). Distinguishing between dots of $\langle 100 \rangle$ and $\langle 1n0 \rangle$ orientations shows that all highly misaligned dots ($\alpha^{\beta_{\text{vor}}} > 10$) are in the $\langle 1n0 \rangle$ orientation and misaligned out of the SL plane as well.